Journal of Manufacturing Engineering, September, 2017, Vol. 12, Issue. 3, pp 179-184

SIMULATION OF MULTIPLE PASS THREE ROLLER BENDING

***Shakil A Kagzi[1] and Harit K Raval[2]**

[1&2]S. V. National Institute of Technology, Surat, Gujarat-395007, India,

ABSTRACT

Three roller bending process is used for the formation of cylindrical and conical shell. Due to bender capacity the required shell dimension cannot be obtained in single pass roller bending. Therefore multiple pass bending is performed. During bending plate is bent to loaded radius. During unloading of plate, the radius of the plate increases due to spring back. Analytical models for estimation of unloaded radius during three roller multiple pass bending process have been reported in literatures. These models are based on the assumptions of constant bend radius to simplify the mathematical formulations. One of the ways to overcome these assumptions is to simulate the process through FEA. In the present work an attempt is made to simulate the multiple pass conical bending in FEA software. The variation in radius of the plate as plate passes through the rollers is noted. The increase in the curvature and the spring back occurring in each pass are seen in the results. The forces are found to increase with each pass during bending operation. The results of final radius were compared with the analytical model available in the literature. Present work may serve as a platform for the research in the estimation of the radius and the forces in multiple pass bending through simulation.

Keywords: *Conical bending, Multiple pass bending, Forces, Radius.*

1.Introduction

Three roller bending process consist of two bottom roller and a top roller. During bending, the bottom rollers are kept at the fixed span. The plate is placed in between the top and the bottom rollers. The top roller is then given the required displacement against the plate. This completes the static bending. Then the bottom rollers are rotated at fixed rotational speed to drive the complete plate across the rollers for the dynamic bending. If the axis of each roller is kept parallel, then the cylindrical bending can be performed. Conical bending can perform by keeping the axis of either or both of the top and the bottom rollers in inclined position (Gnadhi et al. [1]). Generally symmetric inclination is provided to the bottom rollers. The schematic diagram of the conical bending operation is as shown in Fig. 1.

In regards with the forces exerted on the frame during bending process, the analysis for design of machine frame has been reported by Kagzi et al. [2]. Yang and Shima [3] derived variation in radius during static and dynamic cylindrical bending, through an iterative procedure incorporating complex mathematical analysis. Raval [4] reported experimental analysis of forces and spring back for cylindrical bending.Gandhi et al. [5] reported mathematical equations for the top roller displacement during bending for the desired radius.

They [6] also established equation for the desired radius obtained through multiple pass bending. Gandhi [5,6] also reported different roller configuration and mathematical formulation of the spring back for the single pass and multiple conical bending. Chudasama [7,8] had reported the mathematical formulation of forces for the static and dynamic forces during cylindrical and conical bending process.

The mathematical formulations of forces and springback stated above were based on the assumption of the constant bend radius. The radius of the plate was assumed to constant throughout the bending process with a circle tangent to all three rollers. The assumed circle in the reported mathematical mdels is as shown in Fig. 1.

Simulations performed in ANSYS-LS Dyna environment, were reported for asymmetrical three roller bending by Feng et al. [9], to ascertain the position of the lateral rollers for the desired radius. Zeng et al. [10] performed the simulation of conical bending with conical rollers to establish the kinematic contact. Feng et al. [11] used non-compatible rollers for conical bending with an

**Corresponding Author - E- mail: shakil128@gmail.com*

attachment to maintain the velocity of the plate and to increase the accuracy of the geometry. Kagzi and Raval [12, 13] reported simulations to perform the analysis of the forces exerted during single pass cylindrical and conical bending processes by varying different roller configurations.

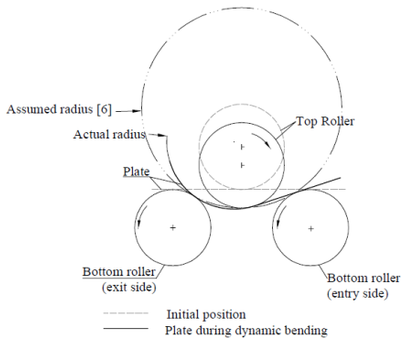

Fig. 1 Schametic diagram of three roller bending

The analytical models reported were based on the assumption of the constant bend radius throughout the bending operation. This bend radius was assumed to be the radius of the circle tangent to all the three rollers. In actual practice, the radius varies along the path of the bending. This assumption can be relaxed mathematically as reported by Yang and Shima [3] which involves complex and iterative mathematical relations. One of the ways to relax this assumption is through the FEA simulation. The simulations reported in the literature are for the single pass cylindrical and conical bending. In the present study the simulation is performed for the multiple pass conical bending operation. The results of the final radius so obtained were compared with the mathematical formulation reported in the literature.

2. Simulation

In the present analysis for multiple pass conical bending was performed in ABAQUS software. For the present simulation of the conical bending the bottom roller was kept inclined at an angle of 3.7º, while the top roller was kept as horizontal. The properties of the plate considered for the simulation is shown in Table 1. The dimension of the segment of the plate was decided based on the mathematical formulation reported by Gandhi et al. [1].

Table 1. Material properties considered for simulation

Material	Yield Strength (MPa)	Strength Coefficient (*K*) (MPa)	Strain hardening exponent (*n*)
IS2062 E300 FE 440	300	695	0.207

The rollers were defined as the rigid bodies and were meshed with rigid shell elements with an average size of 10mm. The plate was defined as deformable body and was meshed with the solid elements of average size of 7.7mm in planer region. The thickness of the plate was kept as 14mm and as the spring back occurs due to the elastic zone across the thickness, denser thickness was kept along the normal region with five elements across the thickness of the plate. The meshed model for conical is shown in Fig. 2(a). As per the reported literature [1], stoppers were also placed on the inner and the outer side of the plate to maintain the required motion of the plate during conical bending. The stoppers were also defined as the rigid body and were meshed with the shell elements with an average mesh size of 10mm. Thus the element size of the deformable body was kept slightly smaller than that of the rigid body as suggested in software manual.

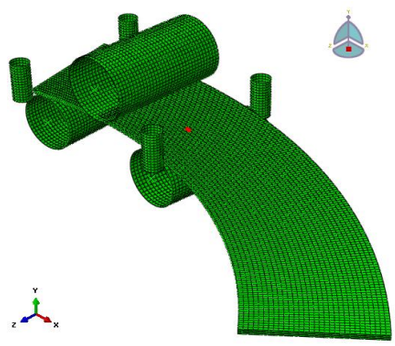

Fig. 2(a) Meshed model for conical bending

For the multiple pass bending operation, the top roller was first displaced at distance of 15mm, to complete the static bending of the first pass. For the second and the third pass the top roller was given the displacement of 10mm and 5mm respectively, during static bending. During static bending the top roller was moved against the plate and the bottom roller was kept steady without rotation.

For the dynamic bending in each pass the bottom rollers were rotated with fixed speed to pass

complete plate across the rollers. The top roller was made free to rotate with the motion of the plate during the dynamic bending. Bottom rollers were rotated with the constant revolution of 6 RPM during dynamic bending in each pass. The deformed plate, with its stress distribution, after the first, second and the third pass is as shown in Fig. 2(b), (c) and (d) respectively

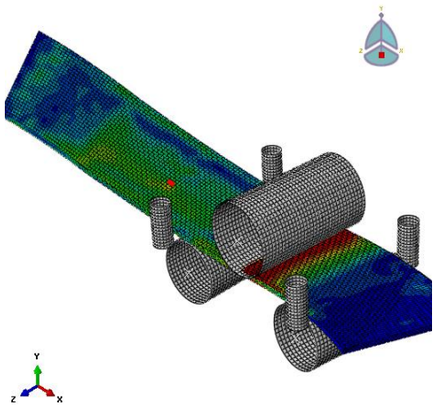

Fig. 2(b) Deformed plate after first pass

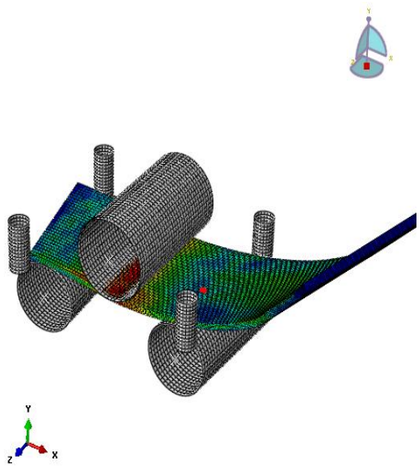

Fig. 2(c) Deformed plate after second pass

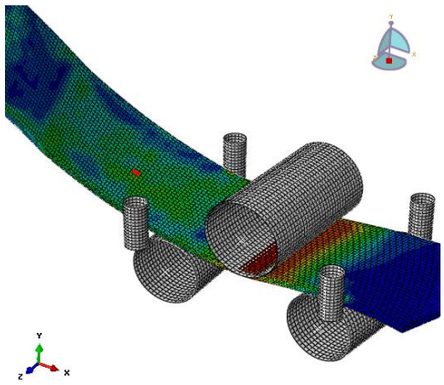

Fig. 2(d) Deformed plate after third pass

The stresses are maximum near the top roller contact. The residual stresses can be observed in the plate as the plate leaves the bottom roller at the exit side. Thus during the second and third pass the effect of residual stresses of the previous was also accounted in the simulation. From these figures it can be noted the final curvature of the plate increases with each pass. The following section discusses about the results obtained from the simulation.

3. Results and discussion

As the plate passes through the rollers, the curvature of the plate increases. The curvature reaches to maximum as it approaches the top roller. The curvature then decreases due to the spring back as the plate leaves the top roller and approaches the bottom roller at the exit side. Practically, it is very difficult to measure the change in radius during the bending operation. However, in literature [6] the loaded radius was assumed to be the radius of the circle tangent to all the three rollers. They [6] determined the relation of unloaded radius after spring back was determined in terms of loaded radius *R*, material properties (strength coefficient *K*, strain hardening exponent *n*), cone angle *ø* and thickness *t* (eq. (1)).

$$R_f = f(R, K, n, t, \phi) \tag{1}$$

$$R, R_f = \frac{abc}{\sqrt{(a+b+c)(b+c-a)(a+c-b)(a+b-c)}} \tag{2}$$

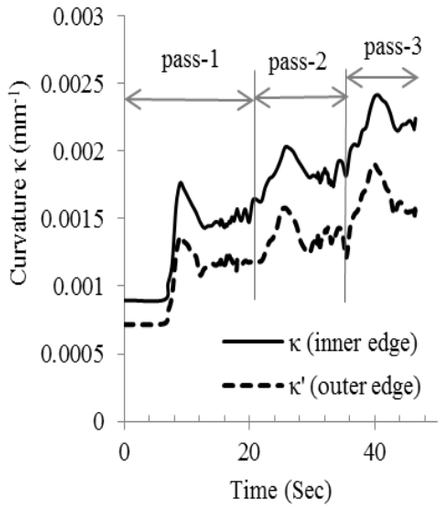

Fig. 3(a) Curvature of plate in different pass

In the present work, actual tensile testing data was used in simulation instead of assuming it as power law. The coordinate of three points on the plate were traced, as the plate moved though the rollers. The variation in radius of the plate can thus be calculated from this traced coordinates by the formulation shown in eq. (2) [14], where letters 'a', 'b' and 'c' indicates linear distances between three points. For calculating the radius at the inner and the outer edge, the coordinates of nodes were considered at the inner and the outer edge of the plate. The plot of the curvature (inverse of the radius obtained) versus time obtained is as shown in Fig. 3(a). Here, κ represent the variation in curvature of the inner edge of the cone being formed during conical bending while κ' represents the variation in curvature at the outer edge. Clearly, the curvature at inner edge is greater than the outer edge during each pass.

It can be seen that the curve is similar to the analytical curvature reported by the Yang and Shima [3] (as shown in Fig. 3(b)), for the cylindrical bending. The curvature is seen to be increasing as the plate approaches the top roller. Near the top roller the curvature of plate is maximum. As the plate moves away from the top roller the curvature of plate decreases. This decrease in curvature is due to the spring back of the plate. When the plate leaves the bottom roller at an exit side it attains constant curvature. This constant curvature is the final curvature obtained in each pass.

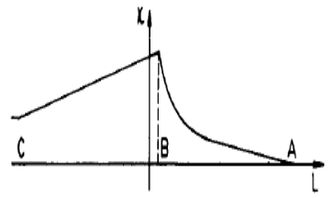

Fig. 3(b) Curvature reported in literature [3]

Table 2. Comparison of results with literature [6]

Pass	Results of Simulation			Results of reported model [6]		Difference	
	R_i (mm)	R_o (mm)	ϕ	R_i (mm)	R_o (mm)	Ri (%)	R_o (%)
1.	674.6	846.9	35	787.8	1057.7	14.3	19.9
2.	554.4	740.1	38	660.4	853.6	16.0	13.3
3.	457.8	639.4	37	566.3	725.1	19.1	11.8

Similar change in curvature can be observed in each pass. The final curvature plate increases with completion of each pass. The radius (an inverse of curvature) so obtained after each pass is compared with the results of the mathematical model for multiple pass bending reported in the literature (Gandhi et al [6]), using the same material properties and the roller configuration. The comparison of the inner and outer radius is as shown in Table II. It is seen that the radius obtained from the simulation are in agreement with reported model with the maximum difference of 20%. It can be seen that the inner radius (Ri) and outer radius (Ro) measured by the reported model [6], is higher than that obtained from the simulation. Unlike, constant loaded radius assumed in literature [6] (dotted line in Fig. 1), simulation being more realistic, variation in the radius was observed with the motion of the plate during bending. The loaded radius obtained is the minimum radius near the top roller contact. This assumed loaded radius is always higher than the actual loaded radius from the simulation. Higher loaded radius leads to higher spring back [1], therefore the final radius obtained from the model is always higher than that obtained from the simulation. Thus the difference in the result is due to the relaxation of the assumption though simulation. The cone angle (ø) varies from 35º to 38º, during three passes. The differences in the radius at the inner and outer edge do not vary significantly during three passes resulting in small variation in cone angle. The

notable decrease in the inner and outer radius is observed.

The forces increases linearly with the displacement of the top roller, followed by the increasing non-linear curve till the maximum displacement of the top roller. With the rotation of the rollers, after static bending, the dynamic bending starts. The force drops during the dynamic bending and then varies in the wavy fashion due to the motion of the plate. This behavior of forces during static and dynamic bending is maintained in each pass. The forces acting on the top roller during the three passes of the conical bending is as shown in Fig. 4. In Fig. 4, (DB) denotes dynamic bending and (S) denoted the static bending.

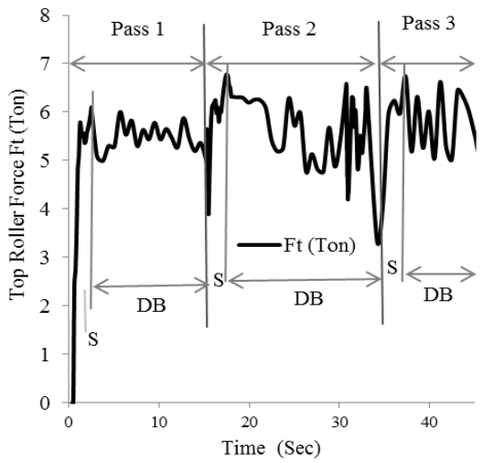

Fig. 4 Force exerted on top roller in each pass

It can be seen that, the maximum static force in each pass is higher than the dynamic force. This difference in forces is due to reversal of the frictional direction during the rotation of the rollers [12]. Also, it is seen from the Fig. 4, that the maximum static force and average dynamic force in each pass is higher than the previous pass. This behavior is due to the fact that due to plastic deformation the yield stress increases after completion of each pass. The top roller is lifted slightly by 2mm to allow the complete spring back of the plate. This results in uneven variation in the load before second and third pass.

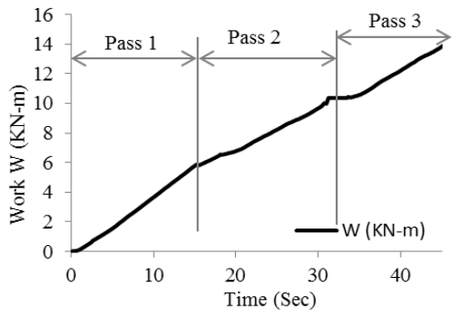

Fig. 5 Work done by the bottom rollers during bending process

The work done by the system is the work done by both of the bottom rollers to drive the plate across the rollers during each pass. From Fig. 5, it is seen that the work done (w) increase linearly in each pass. The slope of the linear curve determines the power consumed during each pass. The power required for first second and third pass is found to be 405.2Watt, 262.6 Watt and 329Watt respectively.

4. Conclusion

The multiple pass bending was simulated successfully in FEA software and different parameters are studied. The bending force is found to increasing in each pass. The radius was found to decreasing in each pass. The radiuses were compared with the reported model and were found to be in agreement with the difference of 20%. The difference is due to relaxation of assumption made in the reported model. In addition of the relaxation of assumption the residual stresses could be accounted for the process in the next pass with the help of this simulation. Thus, FEA proves to be a good tool for simulating multiple pass three roller bending.

References

1. *Gandhi A H (2009), "Prediction of machine setting parameters and roller configuration for continues bending of conical shell on three roller bending machine", Ph. D. Thesis, S. V. National Institute of Technology, India.*

2. *Kagzi S A, Gandhi A H, Raval H K (2012), "Stress analysis of frame structure of three roller bending machine using ANSYS", Journal of manufacturing engineering, Vol. 7(3), 277-283.*

3. *Ming Yang, Susumu Shima (1988), "Simulation of bending type three roller bending process", International Journal of Mechanical Science, Vol. 30(12), 877-886.*

4. *Raval H K (2002), "Experimental and theoretical investigation of bending process", (Vee and three roller bending), Ph. D. Thesis, South Gujarat University, India.*

5. *Gandhi A H and Raval H. K. (2008), "Analytical and empirical modeling of top roller position for three roller cylindrical bending of plates and its experimental verification", Journal of Materials Processing Technology, vol. 197, pp. 268-278, 2008.*

6. *Gandhi A H and Raval H K (2009), "Formulation of springback and machine setting parameters for multi-pass three-roller cone frustum bending with change in flexural modulus", International Journal of Materials Forming, Vol. 2, 45-57.*

7. *Chudasama M K and Raval H K (2013), "An Approximate bending force prediction for three roller conical bending process", International Journal Materials Forming, Vol. 6, 303-314.*

8. *Chudasama M K and Raval H K (2014), "Bending force prediction for dynamic roll-bending during 3-roller conical bending process", Journal of Manufacturing Processes, Vol. 16-2,184-295.*

9. *Feng Zhengkun and Chamliaud Henri (2011) , "Modeling and simulation of asymmetrical three-roll bending process", Simulation Modelling Practice and Theory, Vol. 19, 1913-1917.*

10. *Zeng, Jun, Zhao, heng, Liu and Chamliaud Henri (2008), "FEM dynamic simulation and analysis of roll-bending process for forming of conical tube", Journal of Materials Processing Technology, Vol. 198, 330-343.*

11. *Feng Zhengkun and Chamliaud Henri (2011), "Three stage process for improving roll bending quality", Simulation Modelling Practice and Theory, Vol. 19, 887-898.*

12. *Kagzi S A and Raval H. K. (2014), "An Investigation of forces during roller forming process", Advanced Materials and Research, Vol. 1036, 337-343.*

13. *Kagzi S A and Raval H K (2015), "An Analysis of Forces during Three Roller Bending Process", International Journal of Materials and Product Technology, Vol. 51(3), 248-263.*

14. *Weisstein, Eric W (2016), "Circumradius." From Math World-A Wolfram Web Resource". http://mathworld.wolfram.com/ Circumradius.html.*